BRIEF COMMUNICATION

Luminescence of $CaSO_4:Bi^{3+}$, a Small-Offset Case

D. VAN DER VOORT AND G. BLASSE

Debye Research Institute, University of Utrecht, P.O. Box 80.000, 3508 TA Utrecht, The Netherlands

The luminescence of $CaSO_4:Bi^{3+}(Na^+)$ is reported. The Stokes shift of the $^3P_1 \leftrightarrow {}^1S_0$ emission amounts to about 2000 cm^{-1}. At low temperatures vibrational structure is observed in the emission and excitation spectra with a progression in the symmetric stretching mode of the Bi–O complex. The small Stokes shift and the occurrence of fine structure is ascribed to the positive effective charge of the Bi^{3+} ion on a Ca^{2+} site in $CaSO_4$. © 1992 Academic Press, Inc.

1. Introduction

Recently we have reported on the luminescence of the Eu^{3+} and the Ce^{3+} ion in $CaSO_4$ (*1*). It was shown that the positive effective charge of the Eu^{3+} ion gives rise to a considerable radiationless loss in the excited state of the Eu^{3+} ion. It appears that the Eu^{3+} complex undergoes a considerable expansion in the excited charge-transfer state. This is explained by a model (*2*) which is based on the configurational coordinate model.

For Ce^{3+} we have the reverse situation. The results on $CaSO_4:Ce^{3+}$ have shown that the positive effective charge on the Ce^{3+} ion gives rise to intense luminescence. The Stokes shift of the $5d \rightarrow 4f$ emission of the Ce^{3+} ion in $CaSO_4$ (800 cm^{-1}) is the smallest one reported so far. Furthermore, vibrational structure has been observed in the emission and excitation spectra at low temperatures. These observations point to a weak relaxation in the excited state of the Ce^{3+} ion.

In this study we investigate the influence of an effective charge of the Bi^{3+} ion in $CaSO_4$. The Bi^{3+} ion has $6s^2$ configuration in the ground state and $6s6p$ configuration in the excited state. The luminescence of the Bi^{3+} ion has been studied extensively (*3*). If the Bi^{3+} ion is incorporated tightly in the host material it shows a strong luminescence, vibrational structure in emission and excitation spectra, and a small Stokes shift.

In view of the results for Ce^{3+} in $CaSO_4$ we expect also for Bi^{3+} in $CaSO_4$ a weak relaxation in the excited state (*2*). This has indeed been observed.

2. Experimental

Powders with the composition $Ca_{0.998}Bi_{0.001}SO_4$ and $Ca_{0.998}Bi_{0.001}Na_{0.001}SO_4$ were prepared by usual solid-state techniques (*1*). The following starting materials were used: Bi_2O_3 (Baker Analyzed Reagent), Na_2CO_3 (NH₄)₂SO₄ (both Merck, p.a.), and $CaCO_3$ (Merck, Suprapur). The structure of the reaction products was checked by X-ray powder diffraction using $CuK\alpha$ radiation. All samples were single phase with anhydrite

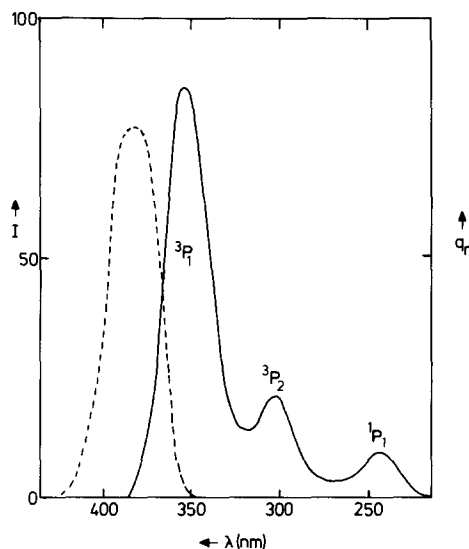FIG. 1. Excitation (solid line, λ_{em} = 410 nm) and emission spectra (dashed line, λ_{exc} = 240 nm) of the luminscence of $CaSO_4$: Bi^{3+} at RT. I gives the relative emission intensity, q_r gives the relative quantum output in arbitrary units. In the excitation spectrum the term symbols of the excited states are indicated.

structure. The luminescence measurements were carried out as described before (1). The emission and excitation spectra were recorded between temperatures from 4.2 (LHeT) to 300 K (RT). The spectra of the two compositions appeared to be identical. The intensity of the Bi^{3+} emission of $CaSO_4$: Bi^{3+},Na^+ was stronger than that of $CaSO_4$: Bi^{3+}. Probably the charge compensation with Na^+ enhances the incorporation of the Bi^{3+} ion in the lattice.

3. Results and Discussion

3.1. RT Measurements

The Bi^{3+} ion in $CaSO_4$ shows intense violet luminescence at RT and below. The excitation spectrum at RT consists of several structureless bands with maxima at 354, 303, and 243 nm (See Fig. 1). These bands are ascribed to transitions from the $^1S_0$ ground state of the Bi^{3+} ion to the $^3P_1$, $^3P_2$, and $^1P_1$ excited states, respectively. The transition $^1S_0 \rightarrow {}^3P_1$ is allowed by spin–orbit interaction. The transition $^1S_0 \rightarrow {}^3P_2$ is forbidden, but becomes allowed by coupling to lattice vibrations. The transition $^1S_0 \rightarrow {}^1P_1$ is fully electric-dipole allowed. However, it is only weakly observed in the excitation spectrum. The diffuse reflection spectrum shows a strong absorption band for this transition. The low excitation intensity is ascribed to the high absorption strength of the $^1S_0 \rightarrow {}^3P_1$ transition, which prevents penetration into the sample. Oomen et al. (4) have observed a similar effect for Sb^{3+} and given the same explanation.

The emission at RT (see Fig. 1), which consists of a band with a maximum at 378 nm, has a decay time of 60 ($\pm$10) nsec and is ascribed to the $^3P_1 \rightarrow {}^1S_0$ transition. At RT the Stokes shift of the $^3P_1 \rightarrow {}^1S_0$ emission amounts to about 2000 cm^{-1}, a fairly low value (3).

3.2. LHeT Measurements

At LHeT the spectra of the Bi^{3+} ion in $CaSO_4$ show structured emission and excitation bands. The Bi^{3+} emission consists of a structured emission band (see Fig. 2) with a maximum at about 400 nm and a decay time of 330 ($\pm$20) μsec. This is typical for the strongly forbidden $^3P_0 \rightarrow {}^1S_0$ transition. Also a small amount of $^3P_1 \rightarrow {}^1S_0$ emission is observed at LHeT.

The $^3P_0 \rightarrow {}^1S_0$ transition starts with a weak zero-phonon line at 384.0 nm, followed by two series of emission lines. The first series consist of lines which are separated by energy intervals of 490 cm^{-1} starting from the zero-phonon line at 384.0 nm (see also Table I). This frequency is due to the symmetrical Bi–O stretching vibration (ν_s). In CaO : Bi^{3+} (5–7) a similar observation was made (ν_s = 480 cm^{-1}). Another vibrational progression in the $^3P_0 \rightarrow {}^1S_0$ transition is much stronger and starts at a false origin at 320 cm^{-1} from the weak zero-phonon line. The $^3P_0 \rightarrow {}^1S_0$ is
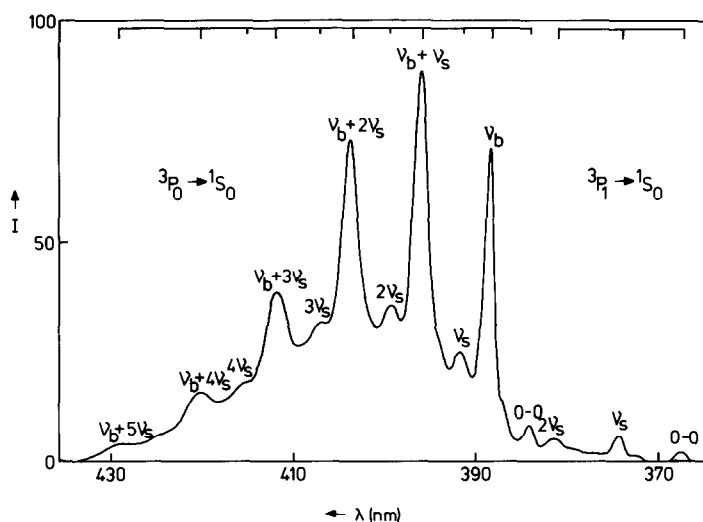
FIG. 2. Emission spectrum of $CaSO_4 : Bi^{3+}$ at LHeT. $\lambda_{exc} = 350$ nm. Progressions in ν_s are indicated at the top of the figure.

strongly forbidden. This explains why the origin is so weak. Obviously the bending mode ($\nu_b = 320$ cm^{-1}) has the correct symmetry to induce intensity in the $^3P_0 \rightarrow {}^1S_0$ transition (6, 7). Similar observations have been made before (8, 9).

TABLE I

DATA ON THE VIBRATIONAL STRUCTURE OF THE $^3P_0 \rightarrow {}^1S_0$ EMISSION OF THE Bi^{3+} ION IN $CaSO_4$ AT LHeT

Wavelength (nm)	E(cm^{-1})	ΔE(cm^{-1})[a]	Assignment[b]
384.0	26040	0	0–0
388.8	25720	320	ν_b
391.6	25540	500	ν_s
396.0	25250	790	$\nu_b + \nu_s$
399.4	25040	1000	$2\nu_s$
404.0	24750	1290	$\nu_b + 2\nu_s$
407.2	24560	1480	$3\nu_s$
411.8	24320	1720	$\nu_b + 3\nu_s$
415.0	24100	1940	$4\nu_s$
420.2	23800	2240	$\nu_b + 4\nu_s$
428.8	23320	2720	$\nu_b + 5\nu_s$

[a] Position relative to origin (0–0).

[b] 0–0, zero-phonon transition; ν_b, Bi–O bending vibration; ν_s, Bi–O stretching vibration.

In the $^3P_1 \rightarrow {}^1S_0$ emission transition a single vibrational progression is observed in the symmetric Bi–O stretching mode. The zero-phonon line at 367.6 nm is followed by emission lines which are separated by an energy interval of 490 cm^{-1}. The $^3P_1 \rightarrow {}^1S_0$ transition is electric-dipole allowed and demands no vibronic coupling to gain intensity. In the emission spectrum of Bi^{3+} in $CaSO_4$ some weak features are present which are not assigned in Fig. 2. Since the spectra are independent of the charge compensating species, we assume that we are dealing with one Bi^{3+} center only. Therefore, these features are ascribed to a coupling of one of the electronic origins ($^3P_1$ or $^3P_0$) with another vibrational mode as observed also by other authors (6–9).

An important parameter which follows from these emission spectra is the Huang–Rhys factor S. The value of S can be derived from the intensity distribution of the lines in the progression. From the $^3P_1 \rightarrow {}^1S_0$ as well as from the $^3P_0 \rightarrow {}^1S_0$ emission spectra it follows that S is about 1.5, pointing to a relatively weak electron–phonon
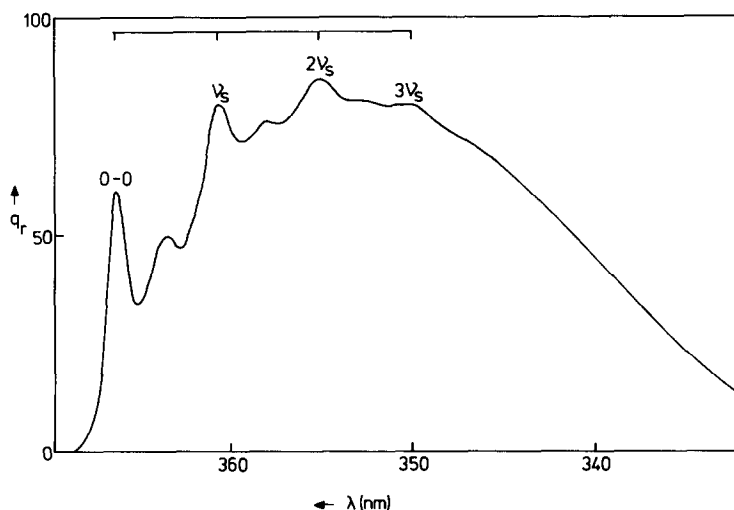
FIG. 3. Excitation spectrum of the emission of $CaSO_4$: Bi^{3+} at LHeT. $\lambda_{em} = 410$ nm. The progression in ν_s is indicated at the top of the figure.

coupling, and hence to a small offset of the excited state parabola.

The excitation spectrum of the Bi^{3+} emission is also structured at LHeT (see Fig. 3). The $^1S_0 \rightarrow {^3P_1}$ absorption transition starts with a zero-phonon line at 366.6 nm. In the emission spectrum this zero-phonon line was observed at 367.6 nm. The difference between these two values may be due to self absorption and/or instrumental imperfection. A vibrational series can be observed with energy intervals of about 430 cm^{-1}. This vibrational mode is ascribed to the Bi–O stretching mode (ν_s). We note that this frequency is lower than in the emission spectra, indicating a weaker bond in the excited state. Similar observations have been made for CaO : Bi^{3+} (6, 7, 9). In between this series of excitation lines some weak features are observed which show also a spacing of 430 cm^{-1}. However, they start at 220 cm^{-1} higher energy than the zero-phonon line. This second series may be due to coupling with a bending vibration with frequency 220 cm^{-1}. However this explanation, includes a large difference between the Bi–O bending

mode in excitation and emission (220 vs 320 cm^{-1}) which is not likely. A second explanation for this series is a transition from the $^1S_0$ ground state to another crystal-field component of the $^3P_1$ level. A Ca^{2+} ion in $CaSO_4$ has site symmetry C_{2v}. A Bi^{3+} ion replacing a Ca^{2+} ion in $CaSO_4$ may have site symmetry C_{2v} also, or even lower because of a distortion of the cation surroundings. In both symmetries the $^3P_1$ state is split three-fold. Therefore it is likely that this second series is due to a transition from the $^1S_0$ level to another crystal-field component of the $^3P_1$ level.

It is of interest to compare the vibronic coupling of the Bi^{3+} ion with lattice vibrations in $CaSO_4$ with that of Ce^{3+} in $CaSO_4$. The Bi^{3+} ion shows a progression in the stretching vibration, whereas the Ce^{3+} ion shows a progression in the bending vibration (1). These observations indicate that the BiO_8 complex expands in the excited state, whereas the CeO_8 complex distorts. The latter effect might be correlated with the Jahn–Teller effect. Aull and Jenssen have proposed a Jahn–Teller effect for the ex-

cited state of Ce^{3+} ion in elpasolite (10), whereas in the case of Bi^{3+} the value of the spin–orbit coupling is larger than that of the electron–lattice coupling (11). This different behavior of Bi^{3+} and Ce^{3+} in $CaSO_4$ is not discussed here any further.

3.3. Test of the Model for Effectively Charged Ions

In this paper we have convincingly shown that the Bi^{3+} ion in $CaSO_4$ shows weak electron–lattice coupling (low S), just as the Ce^{3+} ion. Also in CaF_2; Ce^{3+} (12) a low value of S has been found. Without an effective charge the Bi^{3+} and the Ce^{3+} ion show only vibrational structure in six coordination, but not in eight coordination (3). This shows that the presence of a positive effective charge results in a relatively weak relaxation. This has to be expected from the model presented before (2), since it predicts a weak relaxation for ions with a positive effective charge after excitation into intraionic transitions.

Acknowledgments

References

1. D. VAN DER VOORT AND G. BLASSE, J. Solid State Chem. **87,** 350 (1990).
2. D. VAN DER VOORT AND G. BLASSE, Chem. Mater., **3,** 1041 (1991).
3. See, e.g., G. BLASSE, Prog. Solid State Chem. **18,** 79 (1988).
4. E. W. J. L. OOMEN, W. M. A. SMIT, AND G. BLASSE, J. Phys. C **19,** 3263 (1986).
5. N. YAMASHITA AND S. ASANO, J. Phys. Soc. Jpn. **40,** 144 (1976).
6. A. E. HUGHES AND G. P. PELLS, Phys. Status Solidi A **25,** 437 (1974).
7. A. E. HUGHES AND G. P. PELLS, Phys. Status Solidi B **71,** 707 (1975).
8. A. C. VAN DER STEEN, J. J. A. VAN HESTEREN AND A. P. SLOK, J. Electrochem. Soc. **128,** 132? (1981).
9. A. C. VAN DER STEEN AND L. T. F. DIJCKS, Phys Status Solidi B **104,** 283 (1981).
10. B. F. AULL AND H. P. JENSSEN, Phys. Rev. B **34** 6647 (1986).
11. E. W. J. L. OOMEN, W. M. A. SMIT, G. BLASSE Phys. Rev. B **37,** 18 (1988).
12. S. K. GAYEN AND D. S. HAMILTON, Phys. Rev. I **28,** 3706 (1983).